

Article

Investigating the Impact of Plumbing Configuration on Energy Savings for Falling-Film Drain Water Heat Recovery Systems

Ramin Manouchehri * and Michael R. Collins

Solar Thermal Research Laboratory, Department of Mechanical and Mechatronics Engineering,
University of Waterloo, Waterloo, ON N2L 3G1, Canada; mike.collins@uwaterloo.ca

* Correspondence: ramin.manouchehri@uwaterloo.ca

Abstract: Falling-film drain water heat recovery (DWHR) systems are heat exchangers utilized in residential buildings for recovering energy from greywater. A recent publication by the authors contained a validated model that can be used to predict the performance of DWHR heat exchangers under variable flowrates and temperatures, and this work shows the implementation of the model into Transient System Simulation Tool (TRNSYS) software to perform energy simulations. This work aims to show the different plumbing configurations in which DWHR heat exchangers could be installed, and to simulate their performance under various conditions. The results show that plumbing configuration has a significant impact on energy savings expected from DWHR heat exchangers, and maximum savings are achieved in equal-flow configuration. However, other plumbing configurations provide significant savings, and the mains temperature could dictate which configuration provides higher energy savings.

Keywords: falling-film drain water heat recovery; heat exchanger; TRNSYS; energy simulations; variable plumbing configuration



Citation: Manouchehri, R.; Collins, M.R. Investigating the Impact of Plumbing Configuration on Energy Savings for Falling-Film Drain Water Heat Recovery Systems. *Energies* **2022**, *15*, 1141. <https://doi.org/10.3390/en15031141>

Academic Editor: Jan Danielewicz

Received: 31 December 2021

Accepted: 31 January 2022

Published: 3 February 2022

Publisher's Note: MDPI stays neutral with regard to jurisdictional claims in published maps and institutional affiliations.



Copyright: © 2022 by the authors. Licensee MDPI, Basel, Switzerland. This article is an open access article distributed under the terms and conditions of the Creative Commons Attribution (CC BY) license (<https://creativecommons.org/licenses/by/4.0/>).

1. Introduction

Since 2000, water heating has consistently been the second largest contributor to the total energy consumption in residential buildings in Canada. In the year 2018, 281.3PJ of energy consumed in the Canadian residential sector was attributed to water heating; this represents 17.4% of the total energy consumption and 19.2% of greenhouse gas emissions [1]. Similarly, domestic water heating accounted for 14.8% of the total energy consumption in the residential sector in Europe [2]. Evidently, hot water usage is a significant part of modern housing, and seeking to reduce its impact on the environment is worth investigating.

According to a recent study by Chen et al., an estimated 34.8% of total hot water used in residential buildings within the United States is attributed to showers [3]. Furthermore, on average, drain water holds 80–90% of its thermal energy relative to the mains water supply temperature [4]. Clearly, a significant amount of energy that is consumed towards domestic water heating is not fully utilized during showers, which presents an opportunity to use heat exchangers to recover thermal energy from greywater in residential buildings. This work focuses on the most common type of heat exchanger used for this purpose, namely Falling-Film Drain Water Heat Recovery (DWHR) units.

DWHR heat exchangers consist of a large diameter drainpipe which is wrapped tightly with a coil of smaller tubes. The drainpipe and the tubes are both made of copper. Figure 1 presents a selection of commercially available DWHR heat exchangers, highlighting variations in length, diameter, and coil design for different units. During operation, greywater goes down the drainpipe portion of the heat exchanger, which has a diameter matching the size of the drain stack it replaces. Concurrently, mains water is circulated within the coiled tubes wrapped around the drainpipe which recovers heat from greywater. These heat exchangers are designed to be installed vertically, which implies that greywater forms

a falling-film as it traverses down the drainpipe [5]. This falling-film of water ensures that the entire inner surface area of the drainpipe is covered in water, thus providing the heat transfer area for heat recovery to occur. It is worth noting that horizontal designs for such heat exchangers do not rely on a falling-film, and according to a study by Ravichandran et. al., horizontally installed heat exchangers have lower efficiencies than the ones installed vertically [6]. This study only considers heat exchangers that are designed and rated for vertical installation.

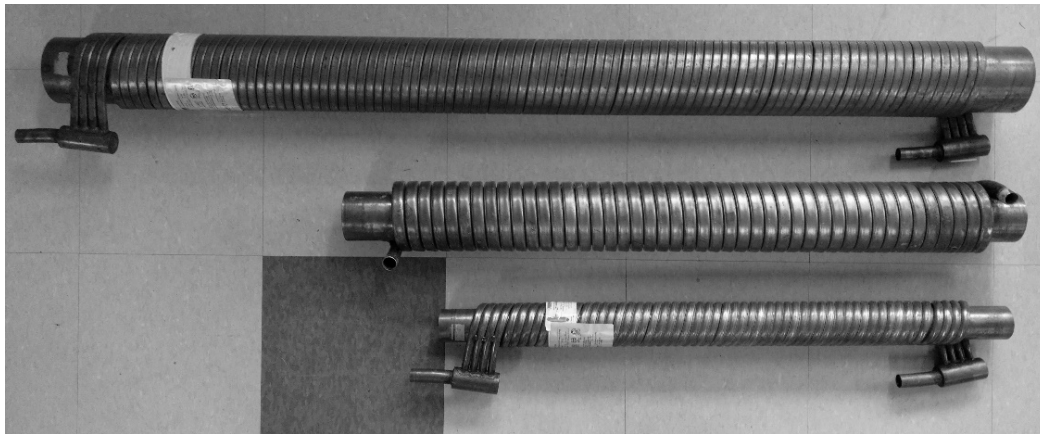


Figure 1. Common designs for falling-film drain water heat recovery (DWHR) heat exchangers.

DWHR systems can be installed in different configurations. Figure 2 shows three variations (A, B and C) which are simplified to only contain a DWHR heat exchanger in addition to a showerhead for water-draw purposes, and each showerhead is equipped with a thermostatic mixing valve. Figure 2A depicts a system where all preheated water from the DWHR system goes to the water heater, Figure 2B depicts a system where all preheated water goes to the mixing valve at the showerhead, and Figure 2C shows a combination of the two previous cases. Lastly, Figure 2D is provided to show the same plumbing system without a DWHR heat exchanger installed.

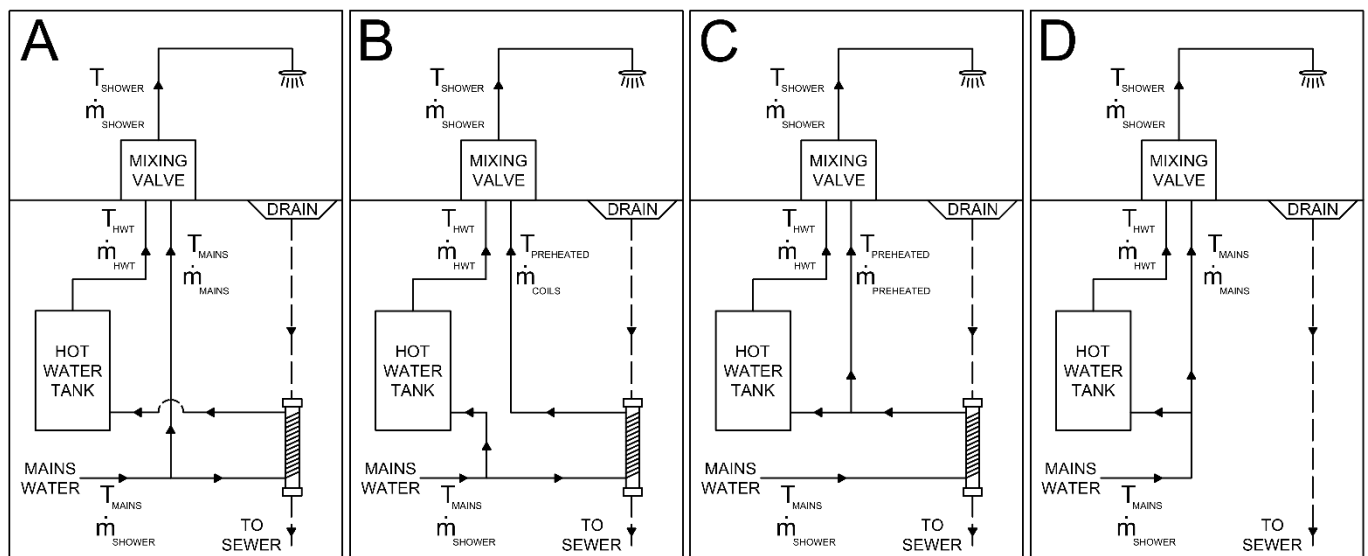


Figure 2. Possible plumbing configurations for DWHR systems in a residential building: (A) depicts a system where all preheated water from the DWHR heat exchanger is fed to the water heater; (B) depicts a system where all preheated water is fed to the mixing valve at the showerhead; (C) is a combination of (A) and (B); and (D) shows the same plumbing system without a DWHR heat exchanger installed.

Configuration C depicts equal flowrates of water through both sides of the heat exchanger, whereas configurations A and B depict unequal-flow conditions. The performance of DWHR systems is a strong function of flowrates [7] and based on the configurations shown, the flowrate of water through the heat exchanger coils is expected to vary based on plumbing configuration to provide the same temperature at the showerhead.

Researchers have been focused on simulating the performance of DWHR heat exchangers under equal-flow arrangements (i.e., config C). This is because the data available on the performance of DWHR heat exchangers is limited to the effectiveness data gathered during the CSA rating process [8]. The rating system is meant to provide a means for comparing different DWHR heat exchangers on an equal basis; it does not and cannot provide any accurate estimates for different configurations in which a heat exchanger could be installed. A study by Slys and Kordana discusses the process for estimating the energy savings associated with different plumbing configurations and highlights the numerous assumptions that need to be made for such calculations [9]. In their work, the authors did not have access to a system model that accounted for varying heat exchanger effectiveness. Without having a model that accounts for the changing effectiveness for the system, there is no way to compare the results numerically or experimentally. This highlights the need for further studies with models that do not rely on assumptions such as a constant effectiveness for the heat exchanger.

It is worth noting that despite being the only configuration covered in standards, configuration C is not always an option, especially in retrofit settings where the plumbing has already been installed and additional modifications are costly. Furthermore, local building codes can impose limitations on which configurations are allowed. For example, configurations B and C are not permitted in Québec, Canada [10]. This restriction is due to the possibility of bacteria growth, such as *Legionella*, in preheated water that bypasses the water heater. In other words, only plumbing setups in which all preheated water is directed to the water heater are allowed, and that limits the allowable configurations to what was shown in Figure 2A. Clearly, assuming that DWHR heat exchangers are always installed and operated under equal-flow conditions is incorrect, and potentially against local codes. Thus, building simulation models must be created to predict performance of such heat exchangers under unequal-flow conditions.

1.1. Model

A series of studies were undertaken at the University of Waterloo to address the limitations in modelling of DWHR systems. Most notably, the impact of varying inlet temperatures [11] and inlet flow rates [12] were empirically characterized, and the combination of all studies were compiled into a model that can predict the performance of a DWHR heat exchanger under steady-state conditions. A recent publication covers the development and validation of the model in detail [13]. The model is validated experimentally and the mean absolute error between model predictions and experimental results is less than 3% for a total of 135 different validation cases performed in the study. The validation temperatures range from 4 to 50 °C, and the volumetric flow rates range from 4 to 20 L/min.

A detailed description of the model and the principles on which those models are based are not repeated here; instead, this study aims to use the aforementioned model to perform energy simulations for DWHR systems installed in configurations depicted in Figure 2. To this end, the model is implemented into Transient System Simulation Tool (TRNSYS) software as a component and used in simulations described in the following sections.

1.2. TRNSYS

TRNSYS was selected as suitable software for simulations because it allows the performance of simulations while accounting for transient behaviour in components such as water heaters. Transient behaviour of DWHR systems is currently being studied and will be added to model in the future.

A TRNSYS simulation works by allowing interaction between different ‘components’ on a timestep-by-timestep basis, and this time step is selected by the user at the beginning of each simulation. Each component consists of ‘parameters’ and ‘inputs’ which are used to generate ‘outputs’ for the components for each time step.

Parameters are relevant values that are used by TRNSYS to simulate a component throughout the simulation period. Parameters are independent of time and remain the same throughout the modelling process. In the context of the DWHR component in TRNSYS, the size of the heat exchanger is a parameter in the simulations. On the other hand, inputs to the simulation are variables that can change as a function of time. The inputs to the DWHR component include the inlet water temperatures and flowrates to the heat exchanger. The simulation then uses the inputs and parameters to generate outputs for the component for each time step. The outputs for the DWHR component include the heat recovery rate, heat exchanger effectiveness, and the outlet temperatures for both streams. A summary of the parameters, inputs, and outputs for the DWHR component are shown in Table 1.

Table 1. Parameters, inputs, and outputs associated with the DWHR component created in Transient System Simulation Tool (TRNSYS) software.

Type	Variable Name	Unit	Notes
Parameter	a	min/L	Regression coefficients taken from the characteristic effectiveness curve for the DWHR unit being simulated.
	b	Dimensionless	
Input	$T_{c,i}$	°C	Inlet water temperature to the coils
	$T_{h,i}$	°C	Inlet water temperature to the drainpipe
	\dot{m}_{coils}	kg/s	Mass flowrate of water through the coils
	\dot{m}_{drain}	kg/s	Mass flowrate of water through the drainpipe
Output	$T_{c,o}$	°C	Outlet water temperature from the coils
	$T_{h,o}$	°C	Outlet water temperature from the drainpipe
	q	kW	Heat recovery rate
	ε	Dimensionless	Heat exchanger effectiveness

Parameters a and b are regression coefficients that are taken from the characteristic effectiveness vs. flowrate curve that is generated during the rating process under the CSA B55.15 standard [8]. Figure 3 shows an example of this characteristic curve, where parameters a and b are determined to be 0.0685 min/L and 1.2796, respectively, and \dot{V} denotes the volumetric flow rate in L/min. The TRNSYS component uses these parameters and the inputs assigned by the user to calculate outputs for each time step.

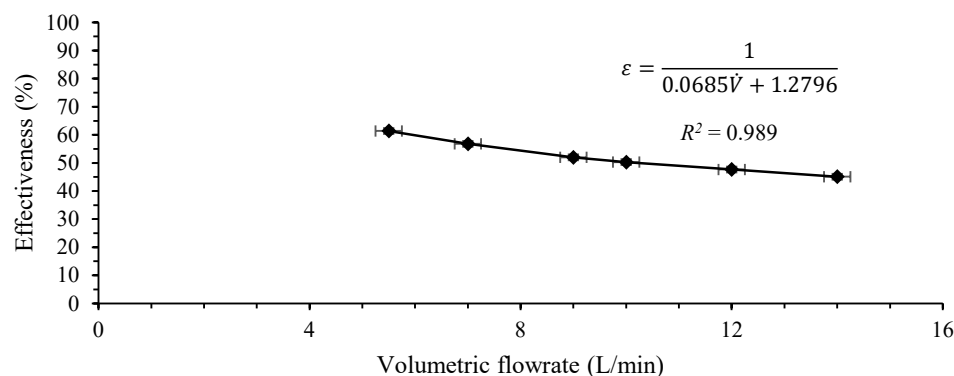


Figure 3. Equal-flow effectiveness vs. volumetric flowrate for a 7.6 cm diameter, 153 cm long DWHR heat exchanger.

2. Materials and Methods

The energy savings associated with a DWHR heat exchanger is highly impacted by the way it is installed in a particular home, and the conditions it is subjected to within the dwelling. The plumbing system within a house is impacted by local codes, the mains temperature depends on the location, and the duration for shower events is decided by the occupants. There are many possibilities for the conditions that a DWHR heat exchanger could be subjected to, and to allow comparison for energy savings under different conditions, a baseline must be established to provide consistency. This baseline is created based on Figure 2 for different plumbing configurations, but prior to running simulations, important simulation constraints, such as the shower condition, the water heater, and the water-draw schedule, must be selected. These key constraints will be discussed.

2.1. Shower Condition

A shower temperature of 38 °C was selected for all shower events. This temperature is based on the temperature used for rating all DWHR systems according to the CSA standard [8].

The flowrate of water through the showerhead is expected to have a significant impact on simulation results, as it would affect both the energy consumption by the water heater, and the energy recovery by the heat exchanger. It is difficult to select one showerhead flowrate to represent all households, as there are many fixtures available on the market, each having its own rated flowrate. In a typical dwelling, this flowrate is also affected by the available water pressure in the plumbing system. Hence, to simplify the matter, three flowrates were selected based on the range of flowrates prescribed by the CSA standard to represent showerheads having low, typical, and high flowrates. These flowrates are 5.5, 9.5 and 14 L/min.

The water draw schedule was chosen for a family of three, with three shower events per day, as noted in Table 2. Shower durations are highly subjective, and the chosen durations were meant to cover both reasonably short and long showers. As these simulations are focused only on savings associated with shower events, no other water draws were added to the daily water-draw schedule. To accommodate the water draws from Table 2, a typical 182 Litre (40-gallon) electric water heater was selected for simulations. The tank volume was found to be sufficient to accommodate all shower durations at all flowrates without depleting the tank. In other words, the shower temperatures do not drop below 38 °C during shower events.

Table 2. Start times and durations for shower events used in the simulations.

Shower Event #	Start Time	Duration
1	6:00 AM	6 min
2	7:00 AM	15 min
3	8:00 PM	9 min

2.2. Electric Water Heater

There are multiple water heaters available for simulation in TRNSYS, and it was crucial to select one that has been validated experimentally. An in-depth study by Allard et al. focused on validating different electric water heaters used in TRNSYS, and the results showed that TRNSYS 'Type 534' accurately depicts the variables of interest, namely the energy consumption and supply temperature during simulations [14]. Type 534 simulates the tank using a nodal approach while accounting for stratification effects. Hence, Type 534 was selected for simulation purposes. This tank was divided into 50 nodes for the simulations, which exceeds the minimum number of nodes recommended by Kleinbach et al. per Equation (1) [15]. Here, N_{FIXED} denotes the minimum number of nodes in the tank, and $Tank_{Turnover}$ is the ratio of daily water draw and total tank volume. $Tank_{Turnover}$ varies

based on the showerhead flowrate used in the simulation; hence, N_{FIXED} was calculated for all flowrates. As a result, the tank was divided into 50 nodes, as this number of nodes satisfies the minimum number of nodes required for all flowrates and having a consistent number of nodes in the tank for all simulations allows fair comparison of the results. Table 3 provides a summary of relevant parameters for the water heater used in all simulations in this study.

$$N_{FIXED} = 45.8 \times (Tank_{Turnover})^{-1.218} \quad (1)$$

Table 3. Parameters used to characterize TYPE 534 hot water tank in this study.

Parameter	Value Used in Simulations	Unit
Number of Nodes	50	Dimensionless
Tank Volume	182 (40)	Liters (Gallons)
Tank Height	105 (41.4)	Centimeters (Inches)
Tank Loss Coefficient	3.5	kJ/(hr·m ² ·K)
Environment Temperature	20 (68)	°C (°F)
Upper Element	3000	W
Lower Element	3000	W

2.3. Mains Temperature

The energy consumption associated with domestic water heating is directly tied to the mains temperature at the location where the water heater is located. To provide a fair assessment of the impact of mains temperature on the energy savings associated with DWHR heat exchangers, a large range of temperatures were required for simulations. The mains temperatures selected for the simulations were 2, 5, 10, 15, 20, and 25 °C.

The energy savings associated with DWHR systems can be looked at from different perspectives, and it is crucial to clarify how savings are presented in this study. It is insufficient to simply compare the magnitude of energy that was recovered by the DWHR system in each simulation, as there are other components present in domestic water heating. Most importantly, there are heat losses associated with the hot water tank, and the rate of heat recovery is expected to impact the losses, as well as how often the heating elements within the water heater must activate to provide auxiliary heat. Thus, it would be more appropriate to compare the total energy consumed by the water heater instead. For this purpose, the total energy consumed by the water heater in configurations A, B and C are compared to the energy consumption in configuration D (see Figure 2) under identical simulation parameters. This allows presentation of the savings in terms of percentages relative to configuration D.

Equation (2) is used to calculate the energy savings as a percentage of total energy consumed in the reference case (configuration D). E_D denotes the total auxiliary energy consumed by the water heater in configuration D, and E_{Sim} represents the total auxiliary energy consumed by the water heater in configurations A, B or C.

$$Energy\ Savings = \frac{E_D - E_{Sim}}{E_D} \times 100 \quad (2)$$

2.4. Heat Exchangers

Four heat exchangers were selected for this study. This selection spans different heat exchanger lengths and diameters. The corresponding characteristic effectiveness vs. flowrate equation obtained using the CSA standard procedure is also provided for each heat exchanger. See Table 4.

Table 4. Characteristics of the DWHR heat exchangers used in simulations.

	Diameter (cm)	Length (cm)	Curve-Fit Generated Using CSA Flow Rates
Heat Exchanger 1	5.1	91	$\varepsilon = \frac{1}{0.1548\dot{V} + 1.7513}$
Heat Exchanger 2	7.6	122	$\varepsilon = \frac{1}{0.0918\dot{V} + 1.3109}$
Heat Exchanger 3	7.6	152	$\varepsilon = \frac{1}{0.0681\dot{V} + 1.2315}$
Heat Exchanger 4	10.2	152	$\varepsilon = \frac{1}{0.0529\dot{V} + 1.2544}$

2.5. Simulation Time Step

Next, appropriate time step was to be determined. Selecting appropriate time steps is crucial for accurate simulations. Smaller time steps often provide higher accuracy at the expense of CPU-time. However, the time domain must be discretized such that all shower events can be appropriately captured by the chosen time step size. To investigate discretization errors, simulations were run for several time step sizes, and for all cases, the energy consumption by the water heater was calculated for a period of a month. A time step of 1 s was used as the reference, and the results from other time steps were compared to the reference case to estimate the discretization error. The results showed that a time step size of 5 min has a discretization error of approximately 17%, which was reduced to below 1% when a 1-min time step was used. Therefore, a time step of 1 min was found to be suitable for simulation purposes.

TRNSYS simulations were set up to perform a month (30 days) of simulation. The results are to be compared using the energy savings metric from Equation (2) for each heat exchanger.

3. Results and Discussion

The results showed that configuration C outperforms the other configurations for all simulations, regardless of flowrate or mains temperature. This is in-line with the expected performance of DWHR heat exchangers, as configuration C has the highest flow rate of water through the heat exchanger's coils during shower events. On the other hand, the mains temperature could dictate which unequal-flow configuration could lead to higher savings. At high mains temperatures, the savings associated with configuration B outpaced those of A, regardless of the heat exchanger being simulated or the showerhead flowrate. Figures 4–6 contain the results for simulations with showerhead flowrates of 5.5, 9.5 and 14 L/min respectively. Each figure contains four plots, which show the energy savings as a function of mains temperature for the three configurations. Note that each point on the plot represents a month of simulation.

It is important to note that significant energy savings can be achieved by installing a DWHR heat exchanger in plumbing systems regardless of the configuration. In situations where the equal-flow configuration is not possible, homeowners should not be discouraged from relying on configurations A or B. Unequal-flow configurations can be thought-of as having a slightly smaller heat exchanger installed relative to the equal-flow configuration, and selecting a larger heat exchanger has a more pronounced impact on energy savings compared to changing the plumbing configuration.

The energy-savings trend for configurations A and B can be explained through closer inspection of the mains side flowrate through the heat exchanger coils for different simulation scenarios. This is best done using the concept of heat capacity ratio, C_r , which is the ratio of heat capacity rates for the heat exchanger, as shown in Equation (3).

$$C_r = \frac{C_{min}}{C_{max}} = \frac{(\dot{m}C_p)_{min}}{(\dot{m}C_p)_{max}} \quad (3)$$

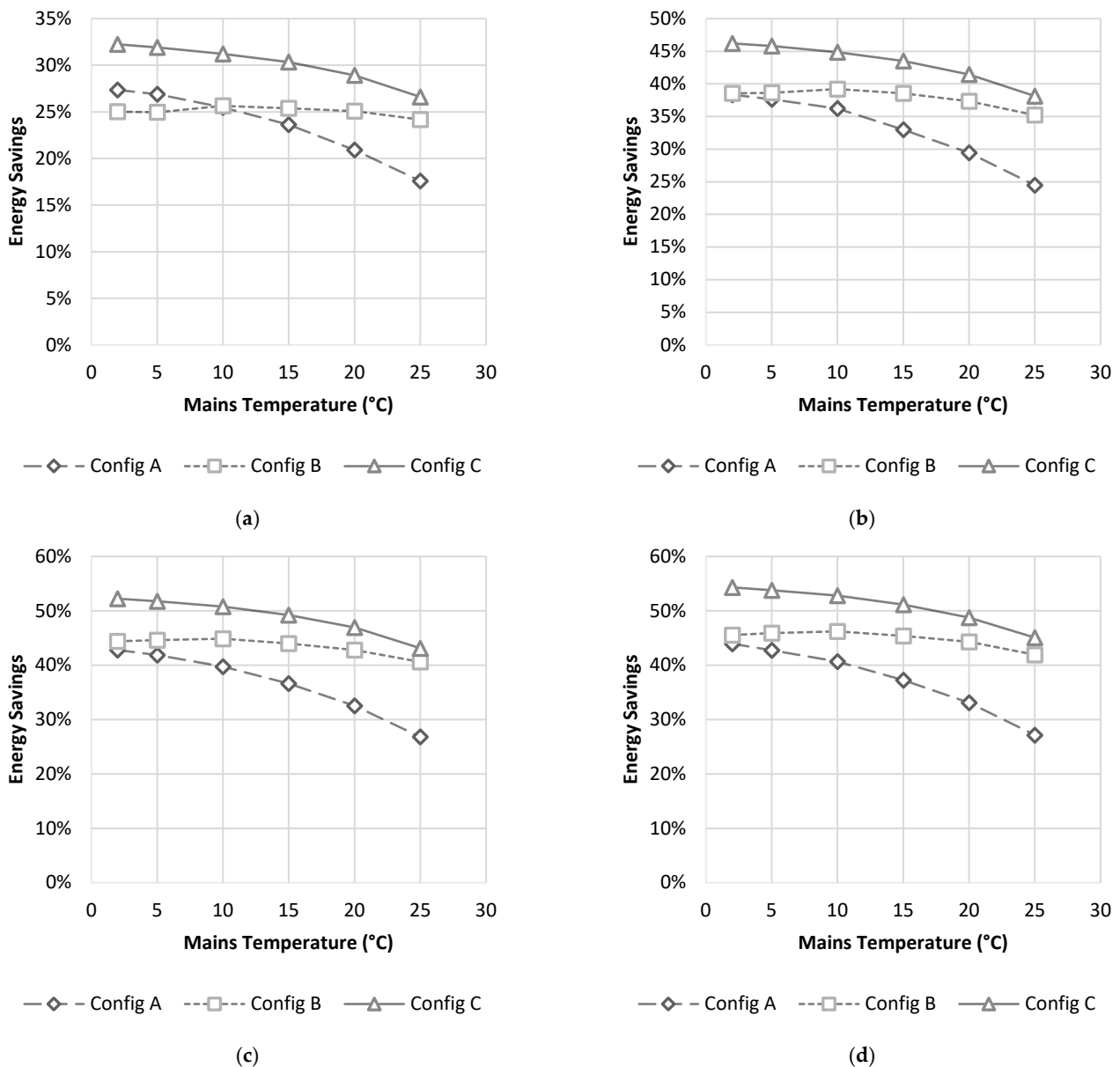
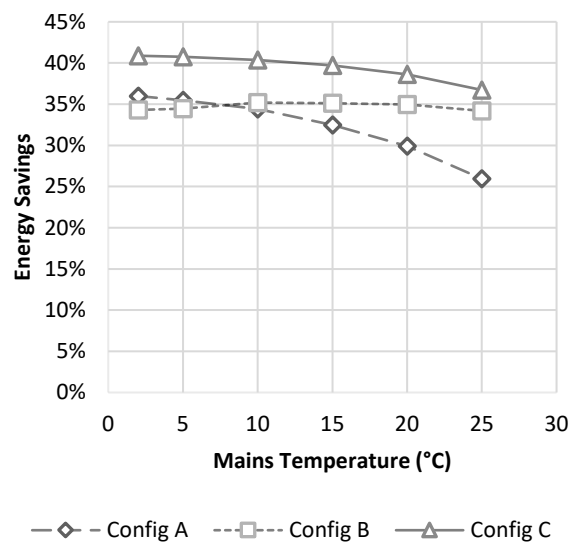
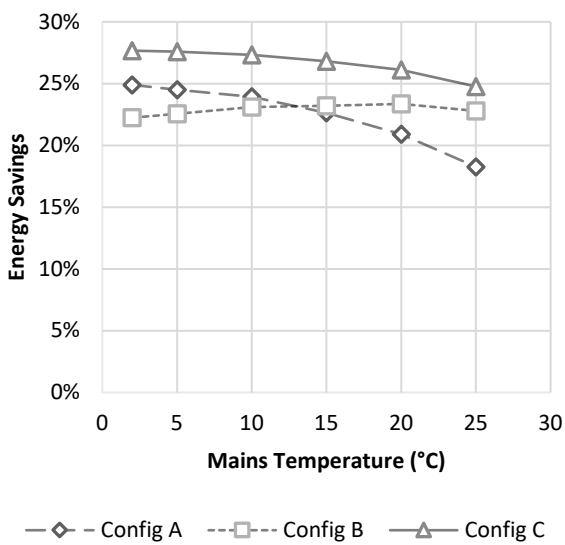


Figure 4. Energy savings as a function of mains temperature for a showerhead flowrate of 5.5 L/min for configurations A, B and C, as labelled. The plots correspond to heat exchanger 1 (a), heat exchanger 2 (b), heat exchanger 3 (c), and heat exchanger 4 (d).

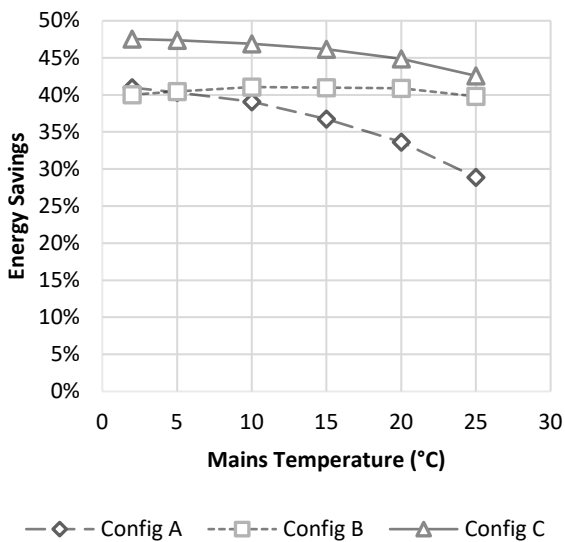
In this equation, C represents the heat capacity rate ($\text{kW}/^\circ\text{C}$), \dot{m} is the mass flow rate (kg/s), and C_p is the specific heat ($\text{kJ}/\text{kg}^\circ\text{C}$). Equation (3) is often used in the ε -NTU method for heat exchanger analysis. For this study, constant properties were used, so Equation (3) can be reduced to a ratio of mass flowrates. Note that the maximum flowrate in this study always corresponds to the flowrate of water at the showerhead fixture, which is equal to the flowrate through the drain side of the heat exchanger. The minimum flowrate corresponds to the lower of \dot{m}_{coils} and \dot{m}_{drain} . The heat capacity ratio, C_r , is nondimensionalized, and is bound between 0 and 1. When the flowrates through the coils and drain are equal (i.e., Config C), C_r will be equal to 1; however, for the other two configurations, \dot{m}_{coils} will always be lower than \dot{m}_{drain} . Thus, C_r can be calculated using Equation (4):

$$C_r = \frac{\dot{m}_{\min}}{\dot{m}_{\max}} = \frac{\dot{m}_{\text{coils}}}{\dot{m}_{\text{shower}}} = \frac{\dot{m}_{\text{coils}}}{\dot{m}_{\text{drain}}} \quad (4)$$

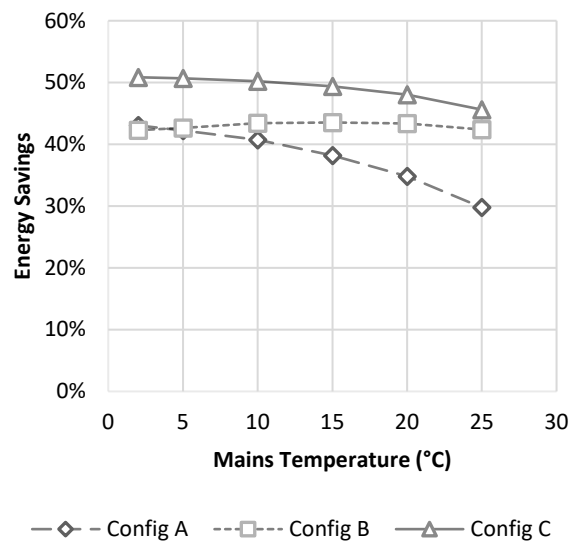


(a)

(b)



(c)



(d)

Figure 5. Energy savings as a function of mains temperature for a showerhead flowrate of 9.5 L/min for configurations A, B and C, as labelled. The plots correspond to heat exchanger 1 (a), heat exchanger 2 (b), heat exchanger 3 (c), and heat exchanger 4 (d).

For this analysis, the heat capacity ratio was calculated for all time steps in the monthly simulation when shower events occurred, and the results for heat exchanger 1 are shown in Figure 7. In this figure, the x-axis contains six sets labelled as 5.5A, 5.5B, 9.5A, 9.5B, 14A and 14B, where 5.5A implies the set of results are associated with configuration A for a showerhead flowrate of 5.5 L/min, and 5.5B implies the set of results are associated with configuration B for a showerhead flowrate of 5.5 L/min, and so on. Each set of results contains six bars, each of which corresponds to a mains temperature (T_m) between 2 and 25 °C, as labelled in the legend. Note that the heat capacity ratios for configuration C are not plotted here, as they are always equal to 1.

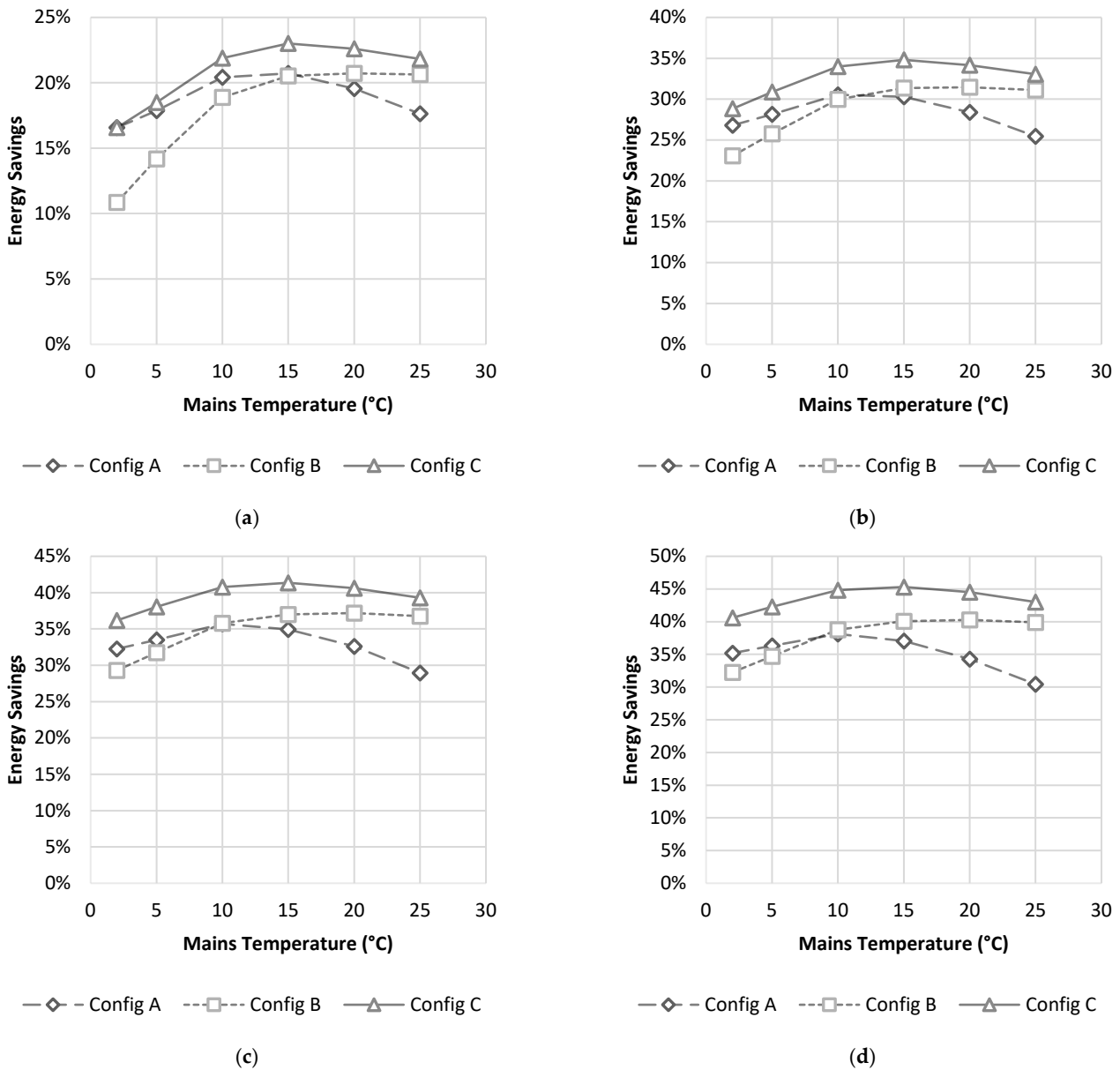


Figure 6. Energy savings as a function of mains temperature for a showerhead flowrate of 14 L/min for configurations A, B and C, as labelled. The plots correspond to heat exchanger 1 (a), heat exchanger 2 (b), heat exchanger 3 (c), and heat exchanger 4 (d).

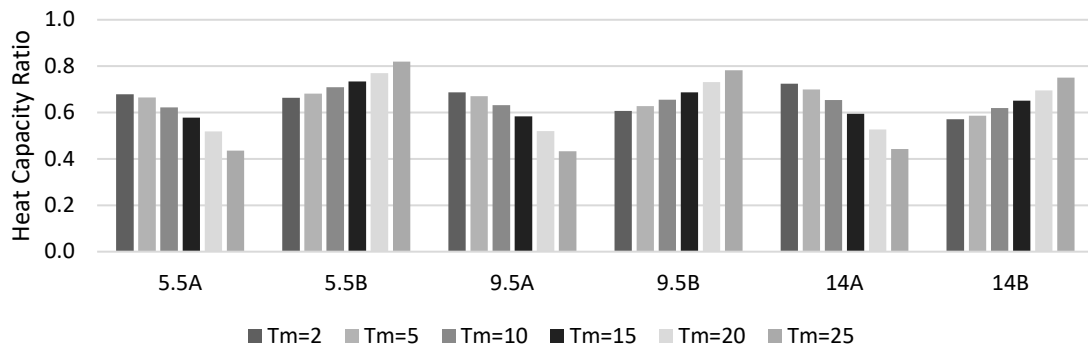


Figure 7. Heat capacity ratios for all simulated cases for heat exchanger 1.

Figure 7 shows that, for configuration A, as the mains temperature was increased in the simulations, the flowrate through the coils was decreased, thereby decreasing C_r . Conversely, configuration B resulted in higher flowrates through the coils as the mains temperature was increased. Figures 8–10 contain the results for heat exchangers 2, 3, and 4, respectively, all of which showed the same trends as Figure 7. Clearly, the mains temperature has a significant impact on \dot{m}_{coils} , which is directly tied to how much energy can be recovered by the heat exchangers. Lastly, the results corroborate what was shown previously in Figures 4–6, where the energy savings for the water heater was shown for different configurations.

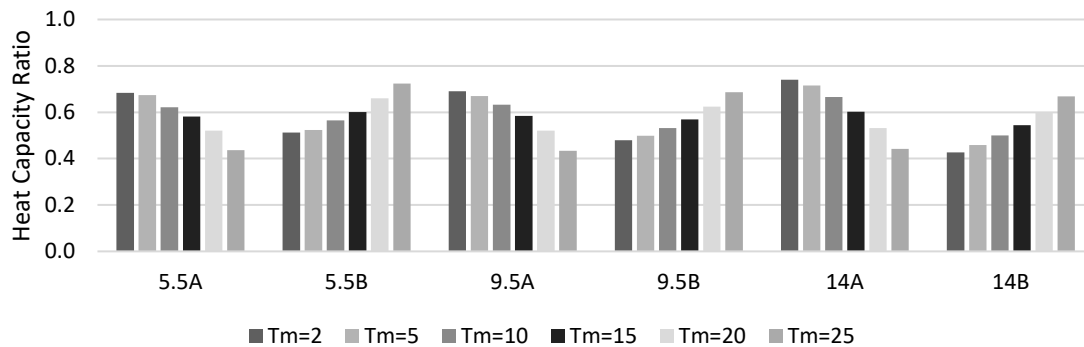


Figure 8. Heat capacity ratios for all simulated cases for heat exchanger 2.

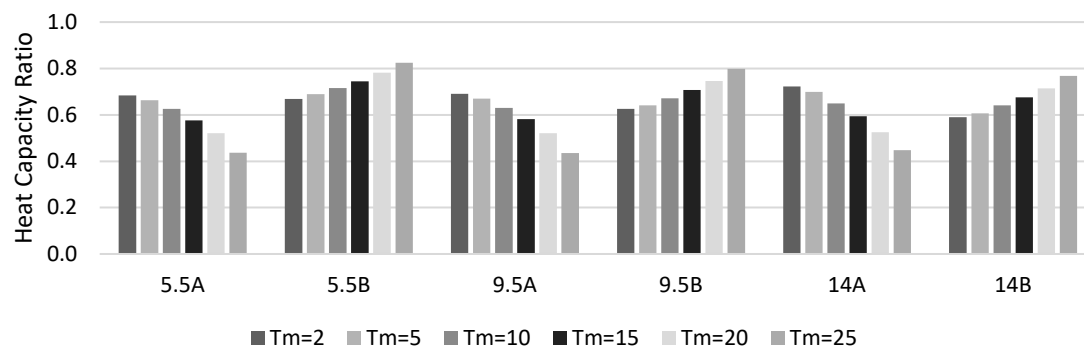


Figure 9. Heat capacity ratios for all simulated cases for heat exchanger 3.

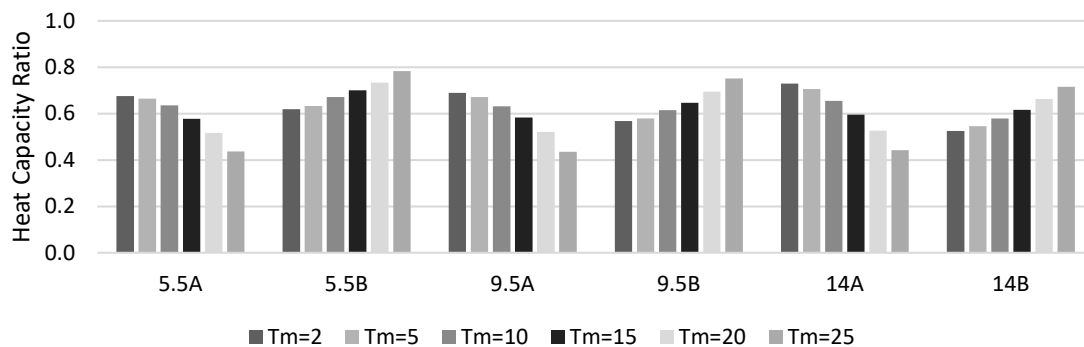


Figure 10. Heat capacity ratios for all simulated cases for heat exchanger 4.

To explain this behaviour, a closer inspection of the plumbing schematic shown in Figure 2 is required. For configuration A, \dot{m}_{coils} is equal to \dot{m}_{HWT} , and as the mains temperature is increased, a higher flow rate of water at T_{mains} would flow directly to the mixing valve; thereby decreasing \dot{m}_{coils} . In other words, the heat exchangers are less utilized in configuration A as the mains temperature is increased and is closer to the prescribed

showerhead temperature. On the other hand, in configuration B, \dot{m}_{coils} is not constrained by \dot{m}_{HWT} , and as the mains temperature is increased, higher flowrates of water would flow through the heat exchanger coils to be preheated. As a result, the heat exchanger is better utilized as the mains temperature is increased in configuration B.

The simulation results highlighted that the mains temperature could dictate the flowrate of water that gets preheated by the heat exchanger in unequal-flow configurations, thereby affecting the energy savings. The mains temperature is based on the location where the plumbing system is located and is expected to vary throughout the year. Designers should be mindful of these facts when implementing a DWHR heat exchanger into a residential plumbing system. The results can also be used by manufacturers as guidelines to improve the design of heat exchangers. Currently, DWHR heat exchangers are rated and sold based on data gathered from equal-flow conditions; hence, they are designed to work optimally in such conditions to be competitive on the market. However, the simulation results showed that if the heat exchangers are installed in unequal-flow configurations, the mass flowrate through the coils could be much lower than the rated conditions. Therefore, the manufacturers are encouraged to adjust the coil diameter to improve heat transfer rates, which increases energy savings when having equal flow rates through the heat exchanger is not an option.

The results from this work showed that plumbing configuration has a pronounced impact on energy savings expected from DWHR heat exchangers. This held true regardless of the heat exchanger size or the prescribed temperature and flowrate at the showerhead. It is noted that reporting simulation results without clarifying the plumbing configuration fails to account for variations in flowrate through the heat exchanger coils and is therefore not an advisable approach. It is the authors' hope that future publications in this field will follow suit and include sufficient information regarding the plumbing setup, such that simulations can be replicated.

Author Contributions: Conceptualization, R.M. and M.R.C.; methodology, R.M.; software, R.M.; validation, R.M.; formal analysis, R.M.; investigation, R.M.; resources, R.M. and M.R.C.; data curation, R.M.; writing—original draft preparation, R.M.; writing—review and editing, R.M. and M.R.C.; visualization, R.M.; supervision, M.R.C.; project administration, M.R.C.; funding acquisition, R.M. and M.R.C. All authors have read and agreed to the published version of the manuscript.

Funding: This research was funded by the Natural Sciences and Engineering Research Council of Canada (NSERC), and the Ontario Graduate Scholarship (OGS) program.

Data Availability Statement: Not applicable.

Conflicts of Interest: The authors declare no conflict of interest. The funders had no role in the design of the study; in the collection, analyses, or interpretation of data; in the writing of the manuscript, or in the decision to publish the results.

References

1. Natural Resources Canada, Comprehensive Energy Use Database, Residential Sector, Canada, Table 2: Secondary Energy Use and GHG Emissions by End-Use. 2020. Available online: <https://oee.nrcan.gc.ca/corporate/statistics/neud/dpa/showTable.cfm?type=CP§or=res&juris=ca&rn=2&page=0> (accessed on 1 October 2021).
2. Eurostat, Energy Consumption in Households. June 2021. Available online: https://ec.europa.eu/eurostat/statistics-explained/index.php?title=Energy_consumption_in_households#Energy_consumption_in_households_by_type_of_end-use (accessed on 2 October 2021).
3. Chen, Y.; Fuchs, H.; Schein, J.; Franco, V.; Stratton, H.; Dunham, C. *Calculating Average Hot Water Mixes of Residential Plumbing Fittings*; Energy Analysis And Environmental Impacts Division Lawrence Berkeley National Laboratory: Berkeley, CA, USA, 2020.
4. Cooperman, A.; Brodrick, J. Drain Water Heat Recovery. *ASHRAE J.* **2011**, *53*, 58–62.
5. Beentjes, I.; Manouchehri, R.; Collins, M.R. An investigation of drain-side wetting on the performance of falling film drain water heat recovery systems, Energy and Buildings. *Energy Build.* **2014**, *82*, 660–667. [[CrossRef](#)]
6. Ravichandran, A.; Diaz-Elsayed, N.; Thomas, S.; Zhang, Q. An assessment of the influence of local conditions on the economic and environmental sustainability of drain water heat recovery systems. *J. Clean. Prod.* **2021**, *279*, 123589. [[CrossRef](#)]
7. Collins, M.R.; van decker, G.W.E.; Murray, J. Characteristic effectiveness curves for falling-film drain water heat recovery systems. *HVACR Res.* **2013**, *19*, 649–662.

8. CSA. *B55.1-15 Test Method for Measuring Efficiency and Pressure Loss of Drain Water Heat Recovery Units*; Canadian Standards Association: Mississauga, ON, Canada, 2015.
9. Sły's, D.; Kordana, S. Financial analysis of the implementation of a Drain Water Heat Recovery unit in residential housing. *Energy Build.* **2014**, *71*, 1–11. [[CrossRef](#)]
10. Régie du Bâtiment du Québec, Branchement des Systèmes de Récupération de Chaleur des Eaux de Drainage: Attention aux Légionelles. March 2013. Available online: <https://www.rbq.gouv.qc.ca/domaines-dintervention/plomberie/interpretations-et-directives-techniques/branchement-des-systemes-de-recuperation-de-chaleur-des-eaux-de-drainage-attention-aux-legionelles.html> (accessed on 6 June 2021).
11. Manouchehri, R.; Collins, M.R. An experimental analysis of the impact of temperature on falling film drain water heat recovery system effectiveness. *Energy Build.* **2016**, *130*, 1–7. [[CrossRef](#)]
12. Manouchehri, R.; Collins, M.R. An experimental analysis of the impact of unequal flow on falling film drain water heat recovery system performance. *Energy Build.* **2018**, *165*, 150–159. [[CrossRef](#)]
13. Manouchehri, R.; Collins, M.R. Modelling the Steady-State Performance of Coiled Falling-Film Drain Water Heat Recovery Systems Using Rated Data. *Resources* **2020**, *9*, 69. [[CrossRef](#)]
14. Allard, Y.; Kummert, M.; Bernier, M.; Moreau, A. Intermodel comparison and experimental validation of electrical water heater models in TRNSYS. In Proceedings of the 12th Conference of International Building Performance Simulation Association, Sydney, Australia, 14–16 November 2011.
15. Kleinbach, E.; Beckman, W.; Klein, S. Performance study of one-dimensional models for stratified thermal storage tanks. *Sol. Energy* **1993**, *50*, 155–166. [[CrossRef](#)]